European Journal of Nuclear Medicine and Molecular Imaging (2019) 46:1605–1615
https://doi.org/10.1007/s00259-019-04336-1

ORIGINAL ARTICLE

[^{18}F]FDG PET/CT in non-union: improving the diagnostic performances by using both PET and CT criteria

Martina Sollini[1] · Nicoletta Trenti[2] · Emiliano Malagoli[3] · Marco Catalano[4] · Lorenzo Di Mento[3] · Alexander Kirienko[3] · Marco Berlusconi[3] · Arturo Chiti[1,5] · Lidija Antunovic[5]

Received: 29 November 2018 / Accepted: 15 April 2019 / Published online: 1 May 2019

Abstract

Purpose Complete fracture healing is crucial for positive patient outcome. A major complication in fracture treatment is non-union. Infection is among the main causes of non-union and hence of osteosynthesis failure. For the treatment of non-union, it is crucial to understand whether a fracture is not healing because of an underlying septic process, since the surgical approach to non-unions definitely differs according to whether the fracture is infected or aseptic. We aimed to assess the diagnostic performance of 2-deoxy-2-[^{18}F]fluoro-D-glucose positron emission tomography-computed tomography ([^{18}F]FDG PET/CT) in the evaluation of infection as possible cause of non-union.

Methods We retrospectively evaluated images of 47 patients treated in our trauma center who, between January 2011 and June 2017, underwent preoperative [^{18}F]FDG PET/CT aiming to exclude infection in non-union. Clinical data, diagnostic examinations, laboratory and microbiology results, and patient outcome were collected and analyzed. [^{18}F]FDG PET/CT images were visually and semiquantitatively evaluated using the maximum standardized uptake value (SUV_{max}). Imaging findings, as assessed by an experienced nuclear medicine physician and an experienced musculoskeletal radiologist, were compared with intraoperative microbiological culture results, which were used for final diagnosis (reference standard). The diagnostic performance of [^{18}F]FDG PET/CT in detecting infected non-union was assessed.

Results Twenty-two patients were not infected, while the remaining 25 had positive intraoperative microbiological results. C-reactive protein (CRP) was within the normal range in 13 cases (five with a final diagnosis of infection) and higher than normal in 25 patients (13 with a final diagnosis of infection). Infection was correctly detected on visual analysis of PET/CT images in 23 cases, while 2/25 infected patients had no significant [^{18}F]FDG uptake and were considered false negatives. In seven cases, [^{18}F]FDG PET/CT showed false positive results; 15/22 disease-free patients were correctly diagnosed. The diagnostic accuracy of [^{18}F]FDG PET/CT in the final diagnosis of infection was 81% (38/47); its sensitivity, specificity, positive predictive value, and negative predictive value were 92%, 68%, 77%, and 88% respectively. The likelihood ratio for a positive test (LR+) was 2.89 and for a negative test, 0.12. Pretest probability of disease was 53%. Post-test probability based on LR+ was 77%.

Conclusion [^{18}F]FDG PET/CT is a promising tool for diagnoses of infected non-unions. Both PET and CT images should be interpreted to achieve a high sensitivity (92%) and a very good negative post-test probability (12%).

Keywords Non-union · Infection · [^{18}F]FDG PET/CT · Diagnostic performance · Fracture-related infections

Electronic supplementary material The online version of this article (https://doi.org/10.1007/s00259-019-04336-1) contains supplementary material, which is available to authorized users.

✉ Lidija Antunovic
lidija.antunovic@humanitas.it

[1] Department of Biomedical Sciences, Humanitas University, Pieve Emanuele, Milan, Italy

[2] Department of Radiology, Humanitas Clinical and Research Center-IRCCS, Rozzano, Milan, Italy

[3] Trauma Center, Humanitas Clinical and Research Center- IRCCS, Rozzano, Milan, Italy

[4] Department of Radiology, Ospedale del Mare, Ponticelli, Naples, Italy

[5] Department of Nuclear Medicine, Humanitas Clinical and Research Center- IRCCS, via Manzoni 56, 20089 Rozzano, Milan, Italy

Background

Prediction of fracture evolution is a major problem in trauma surgery. Correct identification of which type of fracture will develop a non-union and which will heal remains one of the most difficult challenges for any surgeon. The non-union rate is around 5% [1–3]. The factors influencing fracture healing must be addressed using a holistic approach in which both biological (i.e., vascularization, bone growth factors, soft-tissue problems, comorbidities) and mechanical factors (stability of the construct) are carefully evaluated [4, 5]. Infection is among the main causes of non-union and hence of osteosynthesis failure.

The impairment of soft tissues and the exposure of the bone are the main factors that influence the risk of developing infection [6–8], but other factors may also do so, including general clinical conditions and comorbidities, such as diabetes, smoking, and obesity [9, 10].

For the treatment of non-union, it is crucial to understand whether a fracture is not healing because of an underlying septic process. Some patients present clinical signs of infection (e.g., fistula), while in others the clinical diagnosis of infected non-union is difficult. Also, laboratory findings may be equivocal [11]. In these situations, the use of imaging can be a powerful tool for the surgeon that helps to ensure adoption of the most appropriate therapeutic strategy.

In recent years, the use of 2-deoxy-2-[^{18}F]fluoro-D-glucose positron emission tomography-computed tomography ([^{18}F]FDG PET/CT) in infection and inflammation has been extensively evaluated [12]; however, its role in non-union still needs to be fully understood. The aim of this work was to evaluate the diagnostic performance of [^{18}F]FDG PET/CT in the assessment of non-union.

Methods

Patients

We retrospectively evaluated images of patients scheduled for surgical treatment in our trauma center who had undergone a preoperative [^{18}F]FDG PET/CT to exclude an infected non-union between January 2011 and June 2017. Suspicion of infection was based on clinical signs (general: fever; local: swelling, redness, unhealed wounds, fistula appearance, or pain), type of fracture (open fracture or closed fracture with important soft-tissue damage), radiological findings (atrophic or oligotrophic non-union), and laboratory tests [mainly white blood cell count and C-reactive protein (CRP)]. Demographics, clinical data, diagnostic examinations, laboratory and microbiology results, description of surgical treatments, intraoperative microbiological findings, and patient outcome were analyzed. Microbiological culture results for specimens collected during surgery were used as the reference standard to define the final diagnosis. Accordingly, patients were classified as having an infected non-union (intraoperative tissue cultures positive for infection) or not (no evidence of infection on microbiological exams). Overall, 47 consecutive patients (34 male, 13 female) with non-unions of the lower extremities were included in the analyses. Baseline patient characteristics are shown in Table 1. This retrospective study was reviewed and approved by the Ethics Committee.

[^{18}F]FDG PET/CT acquisition protocol

Acquisition and reconstruction protocols are described in detail in the Supplementary Material. In brief, [^{18}F]FDG PET/CT image acquisition was performed according to the European Association of Nuclear Medicine (EANM) guidelines [13]. Images were acquired 60 ± 5 min after [^{18}F]FDG administration, in the fasting state, using an integrated PET/CT scanner, either a Siemens Biograph LS 6 scanner (Siemens, Munich, Germany) equipped with LSO crystals and a six-slice CT scanner, or a GE Discovery PET/CT 690 equipped with LYSO crystals and a 64-slice CT scanner (General Electric Healthcare, Waukesha, WI, USA). All PET images were corrected for attenuation using the acquired CT data. Both scanners are EARL certified (www.eanm.org) and images were processed in order to minimize differences between semiquantitative evaluations.

[^{18}F]FDG PET/CT findings, as assessed by an experienced nuclear medicine physician and an experienced musculoskeletal radiologist, were compared with the intraoperative microbiological findings used for the final diagnosis (reference standard).

Image analysis

[^{18}F]FDG PET/CT images were interpreted visually and semiquantitatively by one experienced nuclear medicine physician (L.A.) and one experienced musculoskeletal radiologist (N.T.). A consensus was reached in the event of discordant opinions. Figure 1 summarizes the criteria used for image interpretation.

Visual analysis

Visual interpretation was performed first by analyzing separately both the PET (visPET) and the CT (visCT) components of the PET/CT. For visPET analysis, both attenuation-corrected (AC) and non-attenuation-corrected (NAC) images were retrieved and evaluated. PET was defined as positive for infection when the following criteria were fulfilled on both AC and NAC images: (i) increased and asymmetrical [^{18}F]FDG uptake in the non-union region compared with the contralateral topographic area, (ii) distinguishable areas of

Table 1 Baseline patient characteristics

	Infected	Non-infected	Overall
Age (years), mean ± SD	51.4 ± 19.2	50.7 ± 19.1	51.7 ± 19.1
Sex			
Female	5	8	13
Male	20	14	34
Side of fracture			
Left	12	11	23
Right	13	11	24
Time between fracture and PET/CT (days, median and range)	302 (36–40,636)	352 (0–1383)	324 (0–40,636)
Previous treatment of fracture			
Conservative (no surgery), *n*	4	1	5
Surgery, *n*	21	21	42
Time between previous surgery and PET/CT (days, median and range)	165 (2–13,353)	202 (9–1223)	190 (2–13,353)
Previous surgery			
Early (≤ 120 days), *n*	8	6	14
Delay (> 120 days), *n*	13	15	28
Time between PET/CT and next surgery (days, median and range)	23 (1–92)	20 (1–85)	16 (1–92)
WBC (10^3/mm^3)	9.2 ± 3.5	8.3 ± 4	8.7 ± 3.6
CRP[a]	8.7 ± 10.5	1.4 ± 2.2	4.7 ± 7.8

WBC white blood cell count, *CRP* C-reactive protein

[a] values missing in nine cases

focal [^{18}F]FDG uptake involving bone fragments of the non-union, and (iii) diffuse and increased uptake, compared with the surrounding soft tissue, along the bone–metallic devices or the bone–bone or bone–graft surfaces. CT images were interpreted as positive in the presence of the following conditions: (a) sclerotic and rounded bone profiles with an important interfragmentary gap (callus fracture sign), (b) absence of trabecular bone structure and increased intramedullary density, with possible Brodie abscess or sequestrations, and (c) increase in soft-tissue density, tumefaction, periosteal effusions, and possible fistula [14, 15]. After the separate evaluation of PET and CT components, an "all-in-one" approach was applied to PET/CT images (visPET/CT). Accordingly, PET/CT images were rated as positive when visual criteria for positivity were present on both PET and CT images. A consensus was reached in the event of discordant opinions (i.e., regarding the presence/absence of PET or CT criteria for positivity).

Semiquantitative analysis

For the semiquantitative analysis, regions of interest (ROIs) were set in the target tissue (i.e., non-union) and in the contralateral muscle (i.e., background). Maximum standardized uptake value (SUV_{max}) within the target tissue ROI was calculated. The ratio between target and background was also computed. Two different semiquantitative approaches were used to rate exams as positive or negative. The first one considered the SUV_{max} in the target region, while the second one evaluated the ratio between the SUV_{max} in the target and in the background (i.e., T/B ratio). Accordingly, exams were defined as positive or negative when the target SUV_{max} or the T/B ratio resulted higher or lower than the cut-off respectively. The cut-off was calculated as the point at which sensitivity and specificity of each measurement were maximized as detailed in the statistical analysis.

Visual plus semiquantitative analysis

The combination of PET/CT visual analysis and semiquantitative analysis was assessed, rating as positive only those exams in which visual PET/CT assessment (visPET/CT) and SUV-based analysis were concordant, as previously proposed [16]. Accordingly, exams were scored as positive when visual criteria for positivity were present on both PET and CT images, and SUV_{max} criteria (i.e., SUVmax or T/B ratio) resulted higher than the cut-off. Conversely, examinations were defined as negative when lacking visPET/CT criteria for positivity, and/or SUV_{max} criteria gave a result lower than the cut-off.

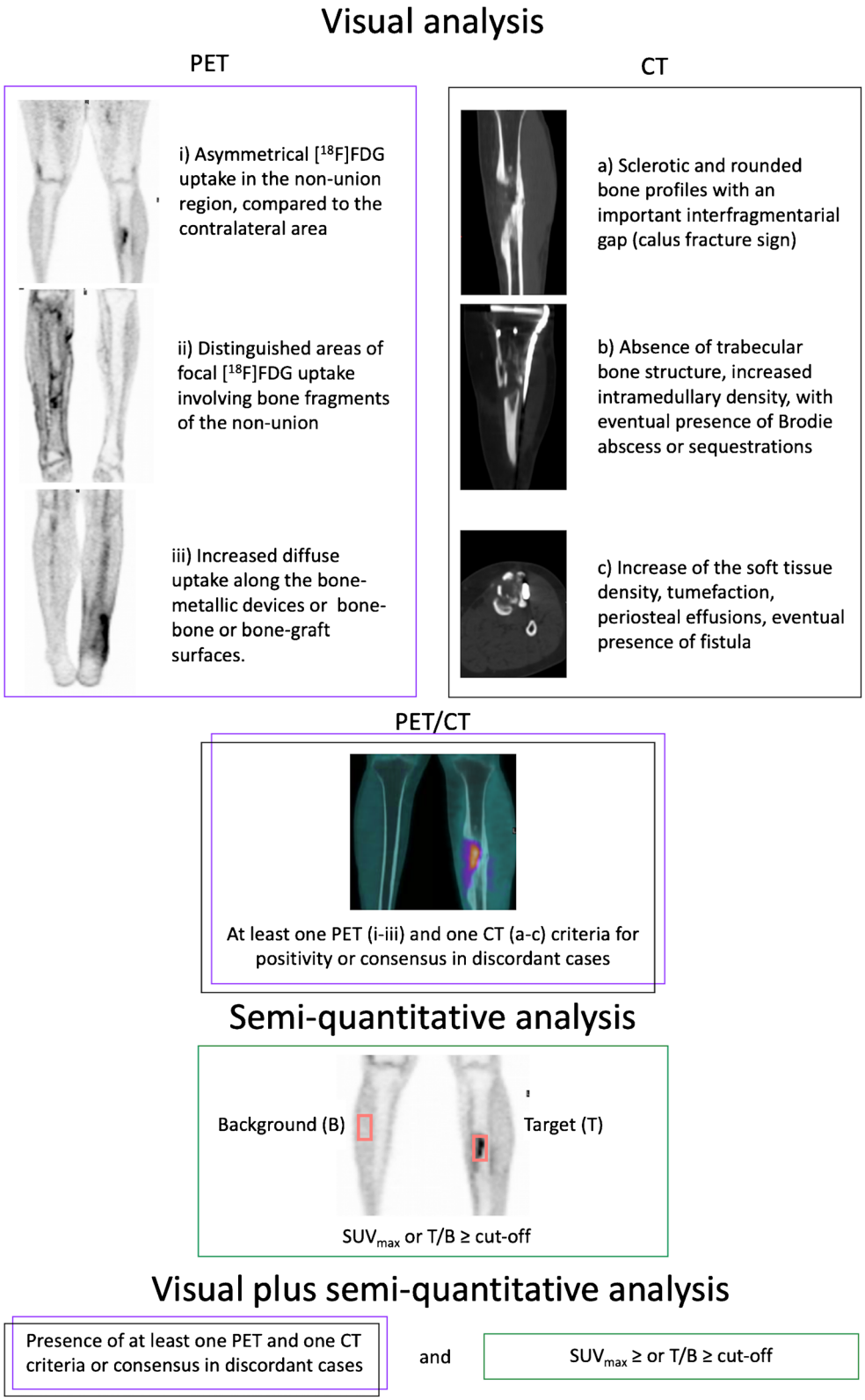

Fig. 1 Schematic representation of the criteria used for image interpretation

Furthermore, the added discriminative power of semiquantitative parameters over PET/CT visual assessment was estimated when discordant findings of PET and CT visual analysis were observed (i.e., PET positive and CT negative or PET negative and CT positive). Therefore, in cases of discordant visual interpretation, the exam was defined as negative or positive when either SUV_{max} or the T/B ratio was respectively lower or higher than the corresponding cut-off value.

Statistical analysis

Patient characteristics were summarized in frequency tables and descriptive statistics were provided for quantitative variables. Each exam was defined as true positive (TP), false positive (FP), true negative (TN), and false negative (FN) if visual, semiquantitative and visual plus semiquantitative analysis agreed or not with the final diagnosis.

Receiver operating characteristic (ROC) curves for target SUV_{max} and T/B ratio were plotted and the corresponding area under the curve (AUC) computed. The Q-point (i.e., the point at which sensitivity and specificity were maximized) on each curve was identified and the corresponding cut-off (i.e., best discriminant ability) for each parameter extracted.

The sensitivity, specificity, positive predictive value (PPV), negative predictive value (NPV), accuracy, and positive and negative likelihood ratios (LR+ and LR− respectively) of [^{18}F]FDG PET/CT in final diagnosis prediction were calculated. The likelihood ratio corresponds to how many times more (or less) likely patients with the disease (i.e., infected non-unions) are to have the index test ([^{18}F]FDG PET/CT) result positive (or negative) than patients without the disease (i.e., aseptic non-unions). Accordingly, [^{18}F]FDG PET/CT results may be equally likely in infected and aseptic non-unions (LR = 1), associated with presence (LR > 1) or the absence (LR < 1) of infection. The LR+ was calculated as the sensitivity/(1 − specificity). The LR- was computed as (1 − sensitivity)/specificity. The pre- and post-test probability and odds — an alternative way of expressing probabilities — were estimated. The pretest probability was defined as (TP + FN)/all cases. The positive post-test probability was computed as TP/(TP + FP). The negative post-test probability was calculated as FN/ (FN + TN) [17]. All metrics were computed for visual, semiquantitative, and both visual and semiquantitative analysis.

Results

Intraoperative tissue cultures were positive for infection in 25 of the 47 patients and negative in the remaining 22. Methicillin-resistant *Staphylococcus aureus* (MRSA) and *Staphylococcus aureus* were the most common pathogens isolated, responsible of six and five infections respectively. CRP was within the normal range in 13 cases (five with a final diagnosis of infection) and higher than normal in 25 patients (13 with a final diagnosis of infection). The pretest probability and the pretest odds of infected non-union were 53% and 1.14 respectively. PET/CT was performed within 4 months from previous surgery in 14 cases (eight of these with a final diagnosis of infection).

Visual analysis

The visPET analysis of the metabolic images, applying the above-mentioned criteria (i–iii), resulted positive in 31/47 patients (23 TP and eight FP) and negative in 16/47 cases (14 TN and two FN). The visCT analysis of the morphological images, applying the above-mentioned criteria (a–c), resulted positive in 32/47 cases (22 TP and ten FP) and negative in 15/47 patients (12 TN and three FN). The "all-in-one" approach, which combined visPET and visCT, rated as positive 30/47 exams (23 TP and seven FP) and as negative 17/47 scans (15 TN and two FN). In the 14 patients who performed imaging within 4 months from the last surgery, visPET/CT resulted positive (both visPET and visCT met criteria for positivity) in ten cases (eight TP and two FP), and true negative in four cases. Particularly, in four patients imaged within the first month after the operative procedure, visPET/CT resulted TP and FP in two and two cases respectively. Among patients with normal CRP, visPET/CT resulted positive in eight of 13 cases (five TP and three FP) and true negative in the remaining five cases. In the 25 patients with elevated CRP, visPET/CT resulted positive in 17 cases (13 TP and four FP) and negative in eight cases (six TN and two FN). Methicillin-resistant *Staphylococcus aureus* (MRSA) and methicillin-sensitive *Staphylococcus aureus* (MSSA) were responsible for infection in the two cases which gave a false-negative result at visPET/CT.

Semiquantitative analysis

Results of the semiquantitative analysis are summarized in Table 2. The best performances were observed for a cut-off of 5.92 for the target SUV_{max} and 2.74 for the target/background ratio. The AUCs for target SUV_{max} and target/background ratio were 0.72 ± 0.08 (95% CI: 0.57–0.84) and 0.66 ± 0.09 (95% CI: 0.51–0.79) respectively. Target SUV_{max} was ≥ 5.92 in 18 cases (15 TP and three FP). In the remaining 29 cases (19 TN and ten FN), SUV_{max} in the target region was lower than 5.92. The target/background ratio was ≥ 2.74 in 32 cases (22 TP and ten FP). In the remaining 15 cases (12 TN and three FN) the target/background ratio was below 2.74. In the 14 patients who performed imaging within 4 months from the last surgery, target SUV_{max} was ≥ 5.92 in four cases (three TP and one FP), while the target/background ratio was ≥ 2.74 in ten cases (eight TP, two FP).

Visual plus semiquantitative analysis

Sixteen visPET/CT positive cases had SUV_{max} in the target higher than 5.92 (13 TP and three FP). The remaining 31 cases were defined negative (12 TN and 19 FN) using the visual plus SUV_{max} criteria. Twenty-five visPET/CT positive cases had a T/B ratio ≥ 2.74 (20 TP and five FP). The remaining 22

Table 2 Results of the semiquantitative analysis of [^{18}F]FDG PET/CT

	Infected patients ($n = 25$)	Non-infected patients ($n = 22$)	Overall ($n = 47$)
SUV_{max} target, mean ± SD (range)	6.18 ± 2.63 (1.91–13.05)	4.50 ± 1.93 (1.13–9.45)	5.40 ± 2.45 (1.13–13.05)
SUV_{max} background, mean ± SD (range)	1.22 ± 0.67 (0.46–3.27)	1.40 ± 0.75 (0.15–1.03)	1.30 ± 0.70 (0.15–3.27)
SUV_{max} target/SUV_{max} background, mean ± SD (range)	6.78 ± 5.73 (1.99–29.0)	4.72 ± 3.93 (1.03–14.33)	5.82 ± 5.03 (1.03–29.0)

SUV_{max}, maximum standardized uptake value

cases were defined negative (17 TN and five FN) using the visual plus T/B ratio criteria.

The application of SUV-based cut-offs to discordant cases resulted in a change in interpretation from positive to negative using the SUV_{max} cut-off in one patient (#33) and from negative to positive using the T/B ratio cut-off in two (#20 and #31) (Table 3).

Diagnostic performances of [^{18}F]FDG PET/CT

The diagnostic performances of [^{18}F]FDG PET/CT using visual, semiquantitative, and combined visual and semiquantitative analysis are reported in Table 4. Figures 2 and 3 respectively show examples of [^{18}F]FDG PET/CT-based confirmatory and negative diagnoses of infected non-union, while Fig. 4 illustrates a case of false-negative PET/CT findings.

Discussion

This study shows that [^{18}F]FDG PET/CT could be a promising diagnostic tool for evaluation of infection as possible cause of non-union. The visual image analysis included the interpretation of both PET and CT components, maximizing the information provided by the exam (i.e., hybrid), as recommended in other clinical conditions within the infection and inflammation domain [18]. Overall, this approach proved to be highly sensitive and satisfactory in terms of positive post-test probability (92% and 77% respectively), as well as remarkably meaningful in terms of negative post-test probability (12%). In our series of patients, PET/CT performed better in ruling out infection in patients with normal CRP, than in ruling in an infection in patients with elevated CRP, confirming that serum inflammatory markers should be carefully interpreted in suspected fracture-related infection (FRI) [11, 19]. As expected for an unspecific test such as [^{18}F]FDG, visPET/CT resulted in a moderate specificity (68%). Specificity increased applying the SUV_{max} cut-off in the target region. Interestingly, the SUV_{max} cut-off identified in our cohort was very similar to that reported by Lemans et al. (5.94 vs 5.9) [20]. This cut-off should be further tested for validation. The combination of the visual approach and semiquantitative analysis was the most balanced in terms of sensitivity and specificity (80% and 77%). The application of the T/B ratio cut-off to cases that were discordant at visual PET and CT analysis improved sensitivity (96% vs 92%) but reduced specificity (64% vs 68%). As previously reported, a useful diagnostic tool for assessment of infected non-unions should balance sensitivity and specificity in order to avoid unnecessary surgery or causing undertreatment of septic delayed unions

Table 3 Results of visual analysis for PET and CT images, the final conclusion on PET/CT, values of the semiquantitative parameters, and the final result of intraoperative cultures in discordant cases

Patient	Time from last surgery	PET visual	CT visual	PET/CT visual	SUV_{max}	T/B ratio	Microbiology
#18	89 days	Negative	Positive	Negative	3.16	1.39	Negative
#20	42 days	Positive	Negative	Negative	5.90	5.90[a]	Negative
#27	264 days	Positive	Negative	Positive	6.34[a]	3.91[a]	*Corynebacterium* species
#28	181 days	Negative	Positive	Negative	4.40	2.41	Negative
#31	n.a.	Negative	Positive	Negative	5.62	2.74[a]	*S. aureus*
#33	106 days	Positive	Negative[b]	Positive	4.50	3.75[a]	*S. aureus*
#44	229 days	Negative	Positive	Negative	2.13	2.53	Negative

T/B target/background

[a] value positive for infection based on the cut-off

[b] CT images positive for soft tissue infection without bone involvement

Table 4 Diagnostic performances of the visual and semiquantitative [^{18}F]FDG PET/CT analyses in predicting fracture related infection

Metric	visPET	visCT	visPET/CT	$SUV_{max} \geq 5.92$	T/B ≥ 2.74	visPET/CT + $SUV_{max} \geq 5.92$	visPET/CT + T/B ratio ≥ 2.74
Sensitivity	92%	88%	92%	60%	88%	41%	80%
Specificity	64%	55%	68%	86%	55%	80%	77%
PPV	74%	69%	77%	83%	69%	81%	80%
NPV	88%	80%	88%	66%	80%	39%	77%
Accuracy	79%	72%	81%	72%	72%	55%	79%
LR+	2.53	1.94	2.89	4.40	1.94	2.03	3.52
LR-	0.13	0.22	0.12	0.46	0.22	0.74	0.26
Post-test probability	74%	69%	77%	83%	69%	81%	80%
Post-test odds	2.88	2.20	3.29	5.00	2.25	4.33	4.00

PPV positive predictive value, *NPV* negative predictive value, *LR* likelihood ratio, *vis* visual

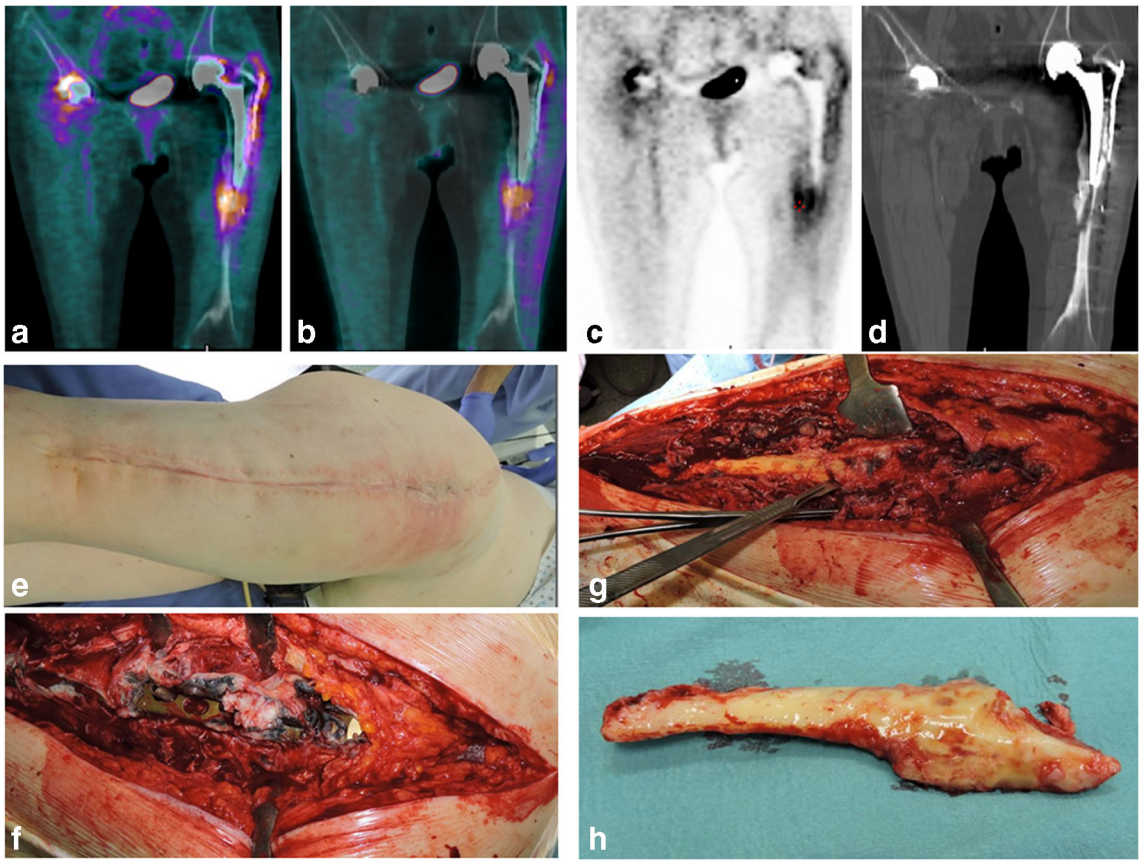

Fig. 2 Case of an 82-year-old female patient (#27) with bilateral post-traumatic hip replacements and left periprosthetic femoral fracture, treated with plate and screws. During follow-up, an oligotrophic non-union was observed, and [^{18}F]FDG PET/CT was performed 264 days after previous surgery, although there were no clear clinical signs of infection (CRP 2.82). Both AC (**a**) and NAC (**b**) PET images show a focal area of increased FDG uptake corresponding to the area of bone non-union on CT images (**c**). PET and CT images were interpreted as positive and negative, respectively applying the visual criteria. A consensus between imagers was reached, and the PET/CT was rated as positive. SUV_{max} in the target was 6.34, and the SUV_{max} target/background ratio was 3.91. Both semi-quantitative parameters were higher than the cut-offs. During surgery, the plate and the screws were removed and sent for microbiological examination (**d**), although there were no macroscopic signs of infection. At plate removal, the area of non-union was found to be next to an ivory-colored cortical bone, which seemed necrotic (**e**, **f**). A wide decortication was performed, with local debridement. The stem was removed together with the entire cemented coat. Plate, screws, and stem were clean; bone tissue was positive for infection [methicillin-resistant *Staphylococcus aureus* (MRSA)]. [^{18}F]FDG PET/CT resulted as true positive applying the visual analysis

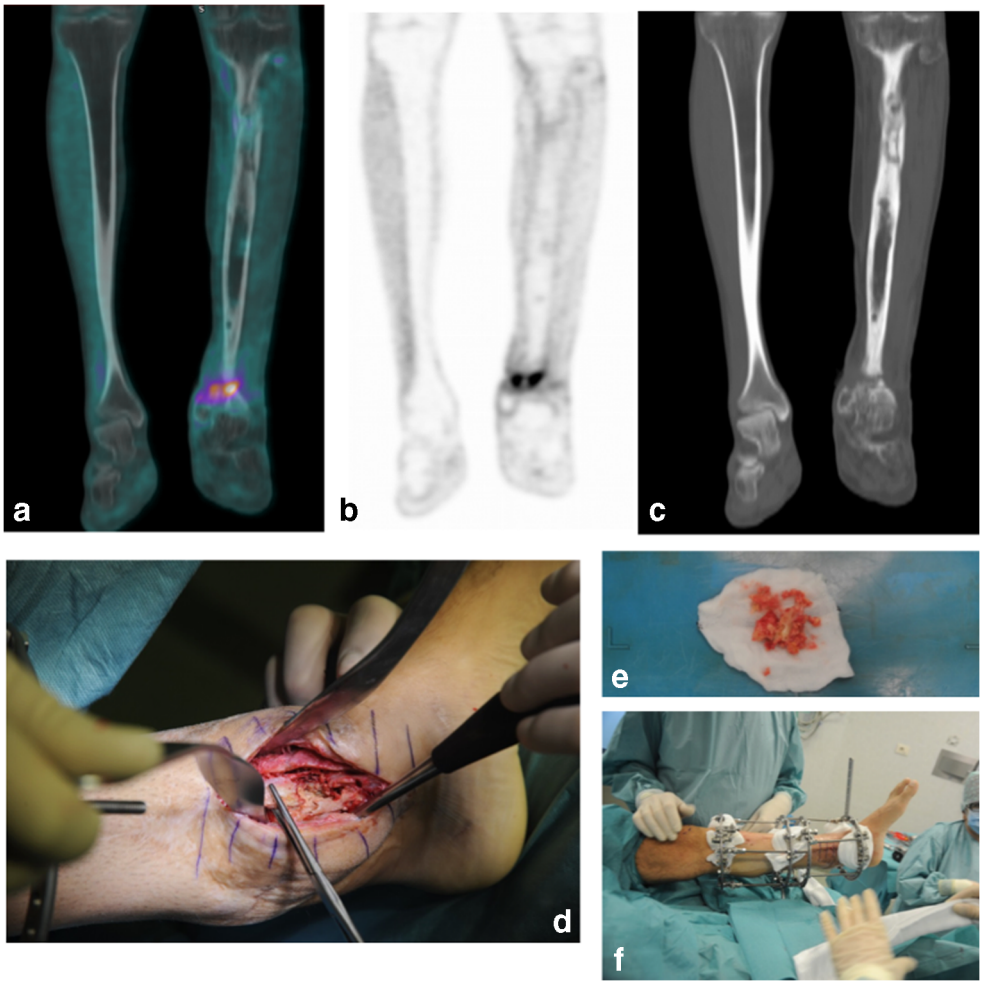

Fig. 3 Case of a 44-year-old male patient (#40), victim of a motorcycle accident that caused him an open left tibia and fibula fracture. One year later, tibia refracture occurred, complicated with infection (*Enterococcus faecalis*). The patient was treated several times with Ilizarov technique. Preoperative [^{18}F]FDG PET/CT images, performed 459 days after previous surgery, showed an area of increased radiotracer uptake (SUV_{max} = 6.1, SUV_{max} target/background ratio = 4.4), in the region of the non-union. During surgery, tibial pilon resection was performed, followed by tibia and fibula osteotomy for left leg lengthening with Ilizarov technique. Microbiology was negative for infection. [^{18}F]FDG PET/CT resulted as false positive applying either the visual and/or the semiquantitative analysis

[21]. However, each non-union should be prudently considered as infected until proven otherwise, since the surgical approach to infected non-union is definitely different from aseptic non-union [19, 22, 23]. Therefore, in non-unions sensitivity should be preferred to specificity. Wenter et al. [16] retrospectively evaluated [^{18}F]FDG-PET in 35 (11 PET standalone and 24 PET/CT) suspected infected non-unions using different visual and semiquantitative approaches. The application of specific criteria for the visual analysis (i.e., asymmetric uptake, focal) increased uptake at the bone–bone, bone–implant, or bone–soft-tissue interface, resulting in a distinct "hotspot"; and uptake along the course of the non-union fracture at least twice the mean uptake of inactive muscle from the contralateral extremity [16, 24, 25]) resulted in high sensitivity and specificity (85% and 86%). However, the application of such strict criteria seems quite difficult when using only PET images. Moreover, these authors' patient population had a rather low pretest probability for infections (37%, calculated on the basis of data in the paper) [16]. More recently, similar findings have been reported in a large cohort of patients with FRI, including non-unions, imaged by [^{18}F]FDG PET/CT. In this series, the high specificity might be related to the high pretest probability for infections (83% calculated on the basis of data in the paper) [20]. In our population the pre-test probability was moderate (53%). Indeed, in our Institution all patients with non-union (not only those with clinical suspicion of infection) are referred for [^{18}F]FDG PET/CT, and all cases are discussed within the "multidisciplinary board for complicated orthopedic patients". Therefore, we had no bias in patient selection. The pre-test probability should be taken into account when interpreting a PET/CT in the infection domains. Very recently, van Vliet et al. [21] retrospectively tested the efficacy and the optimal diagnostic accuracy of [^{18}F]FDG PET/CT in differentiating aseptic and septic lower extremity delayed unions in 30 patients. They found that SUV_{max} was significantly lower in aseptic delayed unions than in septic delayed unions. The best diagnostic performances were observed when setting the SUV_{max} cut-off to 4.0 (sensitivity of 65%, specificity of 77%, and accuracy of 70% with an AUC of 0.747) [21]. Unfortunately, they neither compared semiquantitative analysis to visual assessment nor tested the performances of a normalized SUV_{max} (e.g., target/background ratio). In fact, as is well known, SUV_{max} is affected by many factors [26]. Accordingly, as previously reported, visual

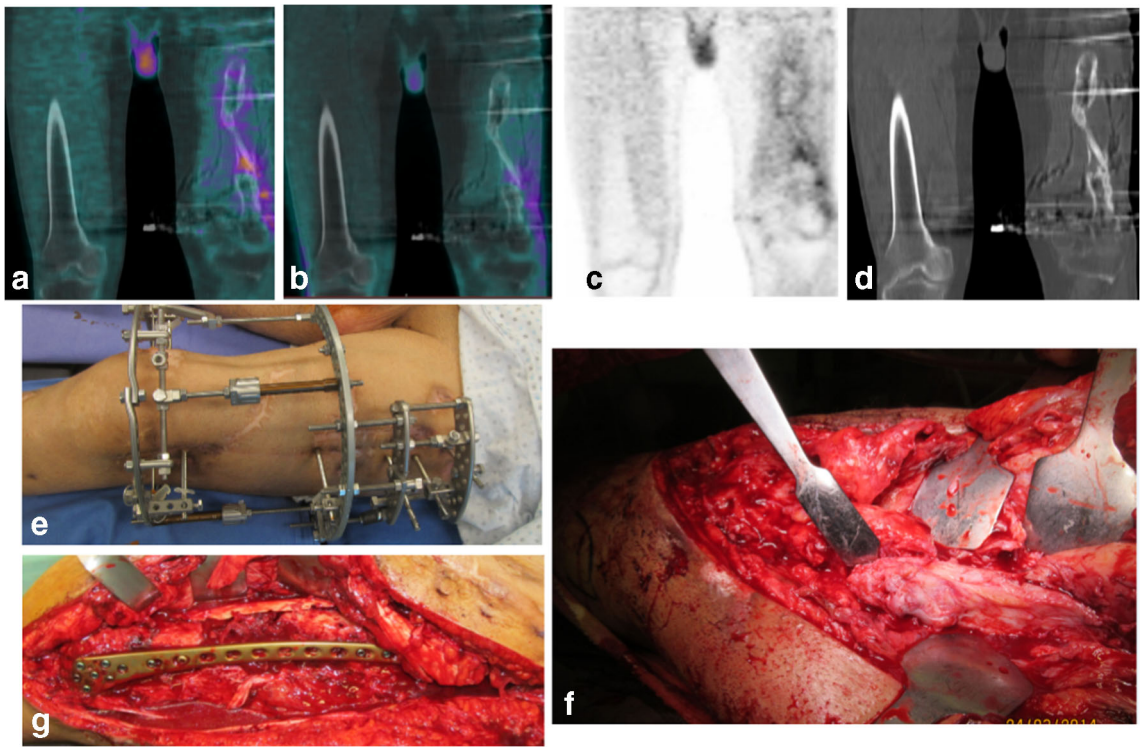

Fig. 4 Case of a 35-year-old male (#9), victim of a road traffic accident with open fracture of left femur. During the next few years he was surgically treated several times for septic non-union. Before the surgical intervention in our center, preoperative imaging was evidencing good transport but difficult healing. Preoperative [^{18}F]FDG PET/CT was performed 137 days after previous surgery; on the PET images there were no significant areas of increased radiotracer uptake, and CT did not show any criteria for positivity. SUV_{max} was 1.91 and tumor/background ratio was 3.97. External fixator was removed. Internal fixation with 4.5 LCP-plate and bone grafting (from iliac crest and musculoskeletal tissue bank) were performed. Microbiological examination evidenced infection with methicillin-resistant *Staphylococcus aureus* (MRSA). [^{18}F]FDG PET/CT resulted false negative applying visual analysis (no criteria for positivity at both PET and CT images) and the target SUV_{max} cut-off. The SUV_{max} target/background cut-off correctly identified the infection

assessment of both PET and CT components is essential while semiquantitative analysis should be carefully used to interpret images, since SUV-based parameters have not yet been validated in the domain of inflammation and infection [18, 27]. Moreover, when the goal is differential diagnosis between infection and inflammation, [^{18}F]FDG PET/CT has not proved indisputably the best suited. Accordingly, radiolabeled leukocyte scintigraphy obtained using SPECT/CT acquisition, combining the high specificity of the tracer with the technological improvements resulting from hybrid equipment (i.e., high spatial resolution) [12], remains the best method in infection, including in the setting of FRI [12, 28–30] even though it does have some drawbacks (e.g., time consuming, highly qualified personnel required for radiolabeling). Notably, radiolabeled leukocyte scintigraphy accuracy is not influenced by the interval between previous surgery and scan [30]. Conversely, a very short interval (< 1 month) between last surgery and [^{18}F]FDG PET/CT has been identified as a major predictor for a false-positive result [20]. In our series, 4 patients were imaged within the first month after operative procedure (2 TP and 2 FP). Other false positive cases occurred in patients imaged after more than 6 months from surgery. However, this was not really surprising, since fracture-healing failure causes a local inflammatory reaction [31] and consequently FDG uptake. In this setting, even the evaluation of morphological images did not result in a remarkable improvement of image interpretation outcome, since as for metabolic images, the mechanical instability (especially when the size of the gap is critical) determines bone alterations [32] resulting in CT abnormalities. As expected, in our series, too, [^{18}F]FDG PET/CT performed better in terms of sensitivity than specificity.

Our study has some limitations. Firstly, it was retrospective and some data (e.g., CRP) were not available for all patients. Secondly, the number of patients included was relatively small. However, in all cases the final diagnosis was microbiologically determined. Thirdly, comparison with other image modalities was not performed.

Conclusions

[^{18}F]FDG PET/CT is a promising tool for diagnoses of infected non-unions. Both PET and CT images should be interpreted to achieve a high sensitivity (92%), and a very good negative post-test probability (12%). The combination

of the visual approach and semiquantitative analysis (i.e., target/background ratio) proved to be the most balanced in terms of sensitivity and specificity (80% and 77%); it also yielded a 80% positive post-test probability but a suboptimal negative post-test probability (26%).

Authors' contributions The manuscript has been seen and approved by all authors, whose individual contributions were as follows: conception and design: MS, LA, NT, MC; patients management and referral: LDM, EM, MB, AK; acquisition of data, analysis, and data interpretation: LA, NT, MC, LDM, EM; drafting the article: MS, LA, AC; final approval of the revised manuscript: MS, LA, MC, NT, LDM, MB, AK, EM, AC.

Raw data are available on specific request to the corresponding author.

Compliance with ethical standards

Conflict of interest A. Chiti received speaker honoraria from General Electric, Blue Earth Diagnostics, and Sirtex Medical, acted as scientific advisor for Blue Earth Diagnostics and Advanced Accelerator Applications, and benefited from an unconditional grant from Sanofi to Humanitas University. All honoraria and grants are outside the scope of the submitted work.

Other authors have non conflict of interest.

Ethics approval The study was approved by the Local Ethics Committee (authorization number 605). A specific informed consent was not required according to Local Ethics Committee rules for retrospective study design.

Abbreviations [^{18}F]FDG, 2-deoxy-2-[^{18}F]fluoro-D-glucose; 3D, tridimensional; AUC, area under the curve; CRP, C-reactive protein; FRI, fracture-related infection; EANM, European Association of Nuclear Medicine; EARL, EANM Research Ltd.; PET, positron emission tomography; PET/CT, positron emission tomography/computed tomography; ROC, receiver operating characteristic; ROI, region of interest; SUV_{max}, maximum standardized uptake value

References

1. Mills LA, Aitken SA, Simpson AHRW. The risk of non-union per fracture: current myths and revised figures from a population of over 4 million adults. Acta Orthop. 2017;88:434–9.
2. Zura R, Mehta S, Della Rocca GJ, Steen GR. Biological risk factors for nonunion of bone fracture. JBJS Rev. 2016;4:e21–212.
3. Zura R, Xiong Z, Einhorn T, Watson JT, Ostrum RF, Prayson MJ, et al. Epidemiology of fracture nonunion in 18 human bones. JAMA Surg. 2016;151:e162775.
4. Giannoudis PV, Einhorn TA, Marsh D. Fracture healing: the diamond concept. Injury. 2007;38(Suppl 4):S3–6.
5. Giannoudis PV, Einhorn TA, Schmidmaier G, Marsh D. The diamond concept — open questions. Injury. 2008;39:S5–8.
6. Karladani AH, Granhed H, Kärrholm J, Styf J. The influence of fracture etiology and type on fracture healing: a review of 104 consecutive tibial shaft fractures. Arch Orthop Trauma Surg. 2001;121:325–8.
7. Alemdaroğlu KB, Tiftikçi U, İltar S, Aydoğan NH, Kara T, Atlıhan D, et al. Factors affecting the fracture healing in treatment of tibial shaft fractures with circular external fixator. Injury. 2009;40:1151–6.
8. Kortram K, Bezstarosti H, Metsemakers W-J, Raschke MJ, Van Lieshout EMM, Verhofstad MHJ. Risk factors for infectious complications after open fractures; a systematic review and meta-analysis. Int Orthop. 2017;41:1965–82.
9. Kyrö A, Usenius JP, Aarnio M, Kunnamo I, Avikainen V. Are smokers a risk group for delayed healing of tibial shaft fractures? Ann Chir Gynaecol. 1993;82:254–62.
10. Parkkinen M, Madanat R, Lindahl J, Mäkinen TJ. Risk factors for deep infection following plate fixation of proximal tibial fractures. J Bone Jt Surg. 2016;98:1292–7.
11. Metsemakers W, Morgenstern M, McNally MA, Moriarty TF, McFadyen I, Scarborough M, et al. Fracture-related infection: a consensus on definition from an international expert group. Injury. 2018;49:505–10.
12. Sollini M, Lauri C, Boni R, Lazzeri E, Erba PA, Signore A. Current status of molecular imaging in infections. Curr Pharm Des. 2018;24:754–71.
13. Boellaard R, Delgado-Bolton R, Oyen WJG, Giammarile F, Tatsch K, Eschner W, et al. FDG PET/CT: EANM procedure guidelines for tumour imaging: version 2.0. Eur J Nucl Med Mol Imaging. 2014;42:328–54.
14. Salih S, Blakey C, Chan D, McGregor-Riley JC, Royston SL, Gowlett S, et al. The callus fracture sign: a radiological predictor of progression to hypertrophic non-union in diaphyseal tibial fractures. Strategies Trauma Limb Reconstr. 2015;10:149–53.
15. Lee YJ, Sadigh S, Mankad K, Kapse N, Rajeswaran G. The imaging of osteomyelitis. Quant Imaging Med Surg. 2016;6:184–98.
16. Wenter V, Albert NL, Brendel M, Fendler WP, Cyran CC, Bartenstein P, et al. [18F]FDG PET accurately differentiates infected and non-infected non-unions after fracture fixation. Eur J Nucl Med Mol Imaging. 2017;44:432–40.
17. Linnet K, Bossuyt PMM, Moons KGM, Reitsma JB. Quantifying the accuracy of a diagnostic test or marker. Clin Chem. 2012;58:1292–301.
18. Erba PA, Lancellotti P, Vilacosta I, Gaemperli O, Rouzet F, Hacker M, et al. Recommendations on nuclear and multimodality imaging in IE and CIED infections. Eur J Nucl Med Mol Imaging. 2018;45:1795–815.
19. Wang S, Yin P, Quan C, Khan K, Wang G, Wang L, et al. Evaluating the use of serum inflammatory markers for preoperative diagnosis of infection in patients with nonunions. Biomed Res Int. 2017;2017:9146317.
20. Lemans JVC, Hobbelink MGG, IJpma FFA, Plate JDJ, van den Kieboom J, Bosch P, et al. The diagnostic accuracy of ^{18}F-FDG PET/CT in diagnosing fracture-related infections. Eur J Nucl Med Mol Imaging. 2019;46:999–1008.
21. van Vliet KE, de Jong VM, Termaat MF, Schepers T, van Eck-Smit BLF, Goslings JC, et al. FDG-PET/CT for differentiating between aseptic and septic delayed union in the lower extremity. Arch Orthop Trauma Surg. 2018;138:189–94.
22. Metsemakers WJ, Kuehl R, Moriarty TF, Richards RG, Verhofstad M, Borens O, et al. Infection after fracture fixation: current surgical and microbiological concepts. Injury. 2018;49:511–22.
23. Mills L, Tsang J, Hopper G, Keenan G, Simpson AHRW. The multifactorial aetiology of fracture nonunion and the importance of searching for latent infection. Bone Joint Res 2016;5:512–9.
24. Love C, Marwin SE, Tomas MB, Krauss ES, Tronco GG, Bhargava KK, et al. Diagnosing infection in the failed joint replacement: a comparison of coincidence detection ^{18}F-FDG and 111In-labeled leukocyte/99mTc-sulfur colloid marrow imaging. J Nucl Med. 2004;45:1864–71.
25. Familiari D, Glaudemans AWJM, Vitale V, Prosperi D, Bagni O, Lenza A, et al. Can sequential ^{18}F-FDG PET/CT replace WBC imaging in the diabetic foot? J Nucl Med. 2011;52:1012–9.
26. Sollini M, Berchiolli R, Delgado Bolton RC, Rossi A, Kirienko M, Boni R, et al. The "3M" approach to cardiovascular infections: multimodality, multitracers, and multidisciplinary. Semin Nucl Med. 2018;48:199–224.

27. Sollini M, Raffaella B, Bandera F, Lazzeri E, Erba PA, Donato PS, et al. Detection of device infection using nuclear cardiology imaging. Ann Nucl Cardiol. 2018;4:52–9.
28. Nepola JV, Seabold JE, Marsh JL, Kirchner PT, el-Khoury GY. Diagnosis of infection in ununited fractures. Combined imaging with indium-111-labeled leukocytes and technetium-99m methylene diphosphonate. J Bone Joint Surg Am. 1993;75:1816–22.
29. Govaert GAM, Glaudemans AWJM. Nuclear medicine imaging of posttraumatic osteomyelitis. Eur J Trauma Emerg Surg. 2016;42:397–410.
30. Govaert GAM, Bosch P, IJpma FFA, Glauche J, Jutte PC, Lemans JVC, et al. High diagnostic accuracy of white blood cell scintigraphy for fracture related infections: results of a large retrospective single-center study. Injury. 2018;49:1085–90.
31. Loi F, Córdova LA, Pajarinen J, Lin T-H, Yao Z, Goodman SB. Inflammation, fracture and bone repair. Bone. 2016;86:119–30.
32. Gaston MS, Simpson AHRW. Inhibition of fracture healing. J Bone Joint Surg Br. 2007;89–B:1553–60.